

Impact of vibrational entropy on the stability of unsolvated peptide helices with increasing length

Mariana Rossi, Volker Blum, and Matthias Scheffler

Fritz-Haber-Institut der Max-Planck-Gesellschaft, Faradayweg 4-6, 14195 Berlin, Germany

Helices are a key folding motif in protein structure. The question which factors determine helix stability for a given polypeptide or protein is an ongoing challenge. Here we use van der Waals corrected density-functional theory to address a part of this question in a bottom-up approach. We show how intrinsic helical structure is stabilized with length and temperature for a series of experimentally well studied unsolvated alanine based polypeptides, Ac-Ala_n-LysH⁺. By exploring extensively the conformational space of these molecules, we find that helices emerge as the preferred structure in the length range $n=4-8$ not just due to enthalpic factors (hydrogen bonds and their cooperativity, van der Waals dispersion interactions, electrostatics), but importantly also by a vibrational entropic stabilization over competing conformers at room temperature. The stabilization is shown to be due to softer low-frequency vibrational modes in helical conformers than in more compact ones. This observation is corroborated by including anharmonic effects explicitly through *ab initio* molecular dynamics, and generalized by testing different terminations and considering larger helical peptide models.

I. INTRODUCTION

Polypeptide helices are a key secondary structure motif in a wide range of proteins [1–3]. It is well known that some amino acids (e.g., alanine) exhibit a stronger helix propensity than others [4–11], but the fact that the helical structure is so abundant in proteins is still intriguing. From a thermodynamic point of view, there are at least two possible limits in which helices compete with other structure prototypes. Towards high temperature, one expects the transition to a random coil [12], which should become entropically favored as the temperature increases. Towards low temperature, however, helices may themselves compete with other enthalpically stable conformations. However, in the most interesting regime, namely intermediate, physiological temperatures, stability may be determined by a delicate balance between enthalpy and entropy [13]. We here unravel this balance quantitatively for the emergence of helical structure in a particularly well studied series of unsolvated polyalanine based peptides Ac-Ala_n-LysH⁺, $n=4-8$ [14, 15]. We consider explicitly not just the helical part of conformational space, but actually the much larger, general low-energy conformational space of the peptides, of which helices are a part. In this paper we show: (i) a

comprehensive search of the conformational space for Ac-Ala_n-LysH⁺, $n=4-8$; (ii) harmonic free energy calculations for several structural candidates; (iii) outlook on the role of anharmonicities in the potential energy surface; and (iv) a theoretical comparison for longer model peptides, considering only helical motifs, with a different termination, in order to clarify the impact of Lys on the soft vibrational modes. Our key finding is that there is a significant vibrational entropic stabilization of helices compared to other, more compact conformers, a contribution that should indeed make a difference in actual proteins as well. This contribution is intrinsic to the helix and should therefore act largely independently, not entangled with environment-dependent terms such as a solvent entropy. Interestingly, an essential role of low-frequency modes is also actively debated in other areas of protein science, related to their function [16–20].

Beginning with the terms that shape the potential-energy surface (PES), known reasons for helix stability include [21, 22] (i) their efficient hydrogen-bond (H-bond) network and increasing H-bond cooperativity with helix length [23–27], (ii) suitably bonded and/or electrostatically favorable termination, for instance the LysH⁺ termination considered here [14, 28–34], and (iii) remarkably, a rather specific favorable contribution of van der Waals (vdW) interactions for α -helices [27, 35]. Clearly, the peptide chain length plays a role: Too short chains have too few and too weak hydrogen bonds for helices to compensate the cost of strain in the backbone [15, 32, 36–38]. In practice, environment effects will necessarily influence helix stability [38–41]. In an aqueous medium, the hydrophobic effect will be prominent [42]. In water-poor conditions, like membranes, helices are frequently observed [43, 44]. Finally, in vacuum conditions, the longer members ($n \geq 8$) of the polyalanine based peptide series studied here assume helical structure in experiment [14, 45, 46]. These helices are stable *in vacuo* even up to extreme temperatures (not expected in solution) [27, 47], or after soft landing on a surface [48].

The potential energy surface also shapes entropy, and thus the effect of temperature T . With increasing T , the conformational entropy of the backbone will favor an unfolded state [12, 22, 49, 50] (so-called “random coil”), while at low T helices may also compete with other, enthalpically more stable conformers. For instance, gas-phase ion mobility spectrometry (IMS) by Jarrold and coworkers [13] showed that the Ac-Ala₄-Gly₇-Ala₄H⁺ polypeptide is helical at $T=400$ K but globular at room temperature. A similar structural change was observed in experiments involving multiply protonated polyalanine in the gas-phase in Ref. [51]. Empirical force-field based simulations by Ma and coworkers [52] of more than 60 small peptides indicate that the *vibrational* entropy (harmonic approximation) could stabilize α -helices or β -hairpins over competing low-temperature conformers. Very recently, Plowright and coworkers [53] used density-functional theory (DFT) including dis-

persion contributions (the B97-D [54] exchange-correlation functional) to suggest that, for a small neutral four-residue peptide, β -sheets and conformers containing 3_{10} helical loops are stabilized by the harmonic vibrational entropy at finite temperatures.

In the present work, we provide independent, unambiguous, and quantitative computational evidence that the vibrational entropy acts to stabilize helical conformers with increasing temperature over more compact, enthalpically competitive structures. The reason, in short, is traced to the softer low-frequency modes of helices, which are also reflected in the dynamics (anharmonic case). We focus on polyalanine-based peptides, since alanine is known to have a high helix propensity both in solution [21, 55] and *in vacuo* [8]. For Ac-Ala_n-LysH⁺ ($n=4-20$) in the gas phase, IMS [15] and first-principles calculations compared to experimental vibrational spectroscopy at room temperature [46] suggest a cross-over from non-helical to helical preferred conformers as a function of polyalanine chain length. For $n=5$ there is a competition between different conformers, while the $n=10$ and $n=15$ conformers are found to be firmly in the helical range [46]. In a previous publication [27] we have quantified, from first principles, the contributions from electrostatics, H-bond cooperativity, and van der Waals interactions on the stability of unsolvated polyalanine-based helices against unfolding. This class of systems is thus an ideal testing ground to clarify the structural competition of non-helical (compact) and helical conformers as a function of chain length also toward the opposite temperature limit (low temperature, folded state). In the following, we address conformational preference of Ac-Ala_n-LysH⁺ *in vacuo* for $n=4-8$, i.e., the length range in which the helical preference at room temperature develops.

Our work is based on an exhaustive prediction of low-energy conformers using DFT and the PBE [56] exchange-correlation functional, corrected to account for long-range vdW interactions [57] (here called PBE+vdW). This level of theory treats accurately, and without system-specific empirical parameters, critical length-dependent contributions such as H-bond cooperativity [23, 25–27] and vdW interactions [27], including their effect on vibrational frequencies and in *ab initio* molecular dynamics.

II. METHODS

Our conformational search strategy, used to find structure candidates of Ac-Ala_nLysH⁺, $n=4-8$, consists of two steps. For a detailed discussion of the search strategy we use here, we refer the reader to Ref. [58]. Both the Lys residue and the C-terminal COOH are considered protonated throughout, as is known to be the gas-phase preference when the N-terminus is capped.[14, 59, 60]

In the first step, we begin by an extensive, unconstrained force field (OPLS-AA [61]) basin-hopping search (using the TINKER package [62]), aiming to simply “list” as many different conformers as possible. The same strategy was employed in Ref. [46], enumerating a huge number of candidate structures: at least 10^5 conformers for each of the molecules in question. Our particular choice of the OPLS-AA force field is not motivated by any other reason than that an input structure “generator” for DFT was needed. In particular, care was taken that small changes to the parameters in the OPLS-AA part of the search do not affect the structure manifold considered in the DFT step below.[58]

In the second step, a wide range of conformers suggested by the force field is fully relaxed using DFT with the PBE+vdW exchange-correlation functional in all-electron total energy calculations (FHI-aims program package [63]). We employ essentially converged numeric atom-centered basis sets and other numerical settings [63, 64] for the relaxations. In detail, the PBE+vdW part of our searches covers 1068, 1000, 800, 800, and 820 conformers for $n=4, 5, 6, 7, 8$, respectively. For $n=6, 7$, and 8 , these numbers are chosen to ensure that at least all conformers identified in the lowest 7 kcal/mol (≈ 0.3 eV) of the force field step are included in the PBE+vdW relaxations. For $n=4$ and 5 , we explored the limits of our search strategy [58]. When comparing locally relaxed minima in PBE+vdW that were obtained by starting from an OPLS-AA local PES minimum structure, we observe a correlation of the relative energy hierarchies, but with a large scatter (max. around 50 meV per residue). Therefore, a large number of conformers must be considered for post-relaxation in PBE+vdW. The comparison also reveals structure-specific force field errors that might otherwise go unnoticed. For example, we observe that OPLS-AA systematically overestimates the energy of 3_{10} -helical structures *in vacuo*. To exclude any unwanted impact of the overestimation of 3_{10} -helices, we performed additional constrained basin-hopping searches in which we forced certain H-bonds of the molecule to remain 3_{10} -helical, again followed by individual, unconstrained PBE+vdW relaxations.

The PBE+vdW relaxed conformers were sorted into “families” according to their H-bond pattern. We define an H-bond to be present when an O acceptor atom is closer than 2.5 \AA to a H donor atom. Within each H-bond family thus defined, small conformational variations are still possible, e.g., by slight bends of the backbone atoms or different rotamers of the LysH⁺ side chain. Typically, the lowest-energy PBE+vdW conformer is found among the family members arising within 5 kcal/mol (0.2 eV) of the lowest-energy force field conformer.

Harmonic vibrational frequencies and intensities were computed from finite differences. The accuracy of the vibrational frequencies calculated in this manner is estimated by analyzing the rotational

and translational modes. These modes should be at zero frequency, and thus the deviation observed gives a limit for the accuracy of the rest of the frequencies. We have not observed deviations of more than 2 cm^{-1} in any calculations. Harmonic free energies were calculated in the harmonic oscillator/rigid body approximation. Vibrational density of states beyond the harmonic approximation were calculated from the Fourier transform of the velocity time autocorrelation function, taken from *ab initio* molecular dynamics trajectories.

For all molecules containing $n \leq 8$ alanine residues and for the Li^+ terminated model structures discussed in this work, no extensive conformational search was performed. These peptides are structure models used specifically for a computer experiment to determine the development of low-frequency vibrational modes with increasing helix length for two different terminations. Their geometries are fully relaxed PBE+vdW structures.

For additional details about these calculations we refer the reader to the Supporting Information.

III. RESULTS AND DISCUSSION

A. Conformational energy hierarchy

Fig. 1 summarizes the energetic ordering of the lowest-energy (PBE+vdW) H-bond families for $n=4-8$, found employing our search strategy. Only the energy of the lowest energy structure belonging to each family is reported, and families are included up to 0.12 eV ($\approx 3 \text{ kcal/mol}$) of the lowest identified minimum of the PBE+vdW PES. α -helical conformers are highlighted in red. The 3_{10} -helical conformer for $n=4$ is highlighted in blue. We define purely α - (or purely 3_{10} -) helical conformers as those where, counting from the N-terminus, all the backbone CO groups at residues i are either connected to NH groups at residues $i+4$ (or $i+3$) or to the LysH^+ side chain (usually the final three or four CO groups at the C terminus). Coordinates and a more detailed analysis of all the geometries shown in Fig. 1 are given in the Supporting Information.

The conformer associated with the lowest-energy PES minimum for $n=4$ is rather small, connecting almost all its backbone CO groups to the LysH^+ termination. The remaining H-bond at the N-terminus is bifurcated, comprising an α - and a 3_{10} -helical H-bond. This conformer could therefore be classified as the smallest possible α -helical prototype in this series. In contrast, the lowest-energy PES minima for $n=5$ and 6 are *not* simple helices. Each contains an “inverted” H-bond where one CO group points to the N-terminus and its connecting NH group points to the C-terminus, producing more compact structures. In Fig. 1, these bonds are highlighted in yellow

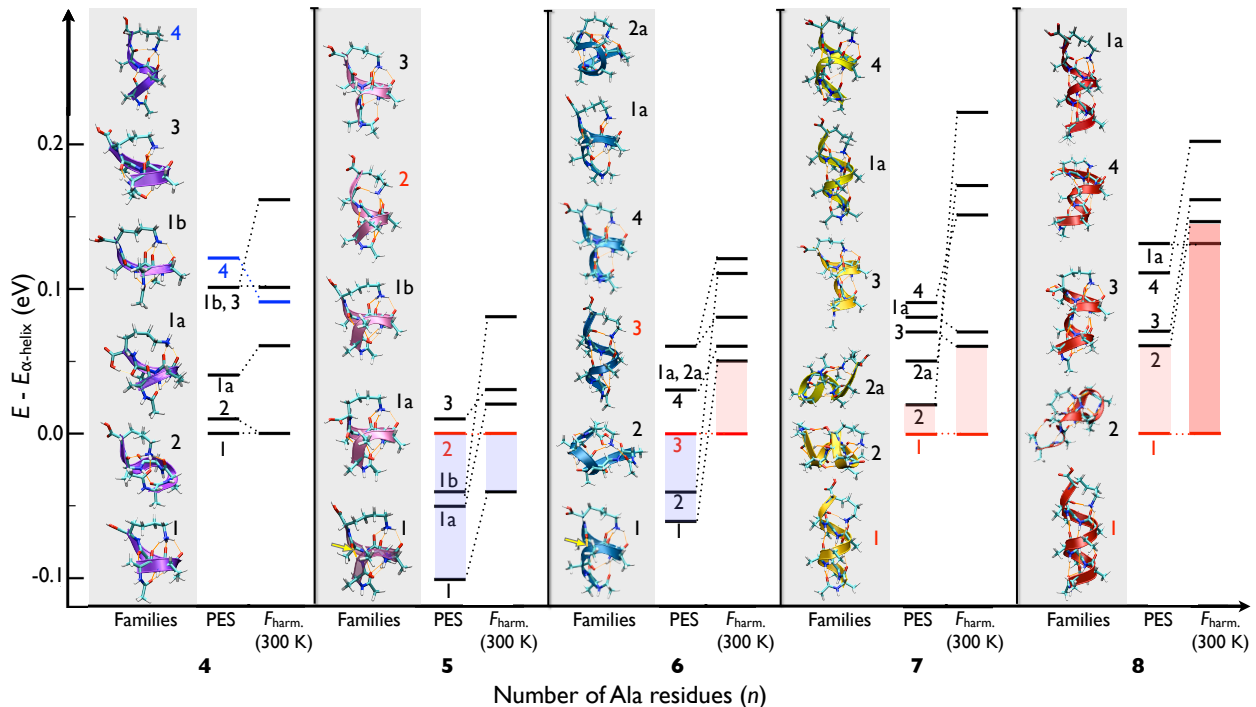


FIG. 1: Energy hierarchies (thick horizontal bars), obtained with the PBE+vdW functional, for the low-energy H-bond families of Ac-Ala_n-LysH⁺, $n=4-8$. For each n , we include the conformer representatives of the lowest-energy families up to 0.12 eV from the global minimum, as defined by local minima of the PBE+vdW potential-energy surface (PES). We also show their hierarchy after adding the corrections for the harmonic vibrational free energy $F_{\text{harm.}}$ at $T=300$ K. Numbers labeling each family, as well as colored structural representations are shown. The placement of the structure pictures in the shaded gray areas is not directly related to the energy axis (y axis), which applies strictly only to the horizontal bars. For these, the α -helical conformer of $n \geq 5$ is chosen as the reference (zero) energy. For $n=4$, Family 1 is taken as the reference. α -helical conformers are highlighted by red bars. The 3_{10} -helical conformer for $n=4$ is highlighted by blue bars. The shaded areas in the energy hierarchies indicate the energy difference between the α -helix and the nearest non-helical conformers.

and pointed to by an arrow. For $n=5$, we have previously denoted this conformer as “g-1” [46]. For $n=7$ and 8, the lowest-energy PES minima correspond to α -helices. In each case, they are closely followed by a conformer that we characterize as compact/globular (Families 2 of $n=7$ and 8, with an energy separation of 20 and 60 meV respectively). Thus, we already observe a cross-over with peptide length to α -helical lowest-energy minima of the PES at $n=7$. However, based on the energy hierarchies of the structures of the local PES minima alone, one would not expect a purely helical ensemble of conformers at room temperature at $n=7$ or 8. Simple Boltzmann factors would indicate a mix of structure candidates. Yet, the experimental work by Kohtani and Jarrold [15]

does indicate a complete room-temperature structural cross-over at $n=8$ at the latest, albeit based on a completely different line of reasoning (water adsorption behavior of “helical” versus “globular” conformers).

For the low-energy conformers in Fig. 1, we also compute and show in the same figure the impact of the vibrational free energy at room temperature ($T=300$ K) in the harmonic approximation [74]. Remarkably, the relative stability of the α -helices is systematically enhanced by the vibrational free energy contribution for *all* n . For $n=5$ and 6 the α -helical conformers move down in energy with respect to the (non-helical) lowest energy PES minimum. For $n=7$ and 8 the α -helices now become the isolated minima. In detail, we observe:

- For $n=8$, the energetic interval between the α -helical lowest energy conformer and the nearest globular one (red shaded areas) now amounts to 0.14 eV. The additional Family 1a at 0.13 eV is another α -helix with a slightly modified terminating H-bond network. With the vibrational free energy included, the energy hierarchy is thus consistent with the experimental claim that α -helices dominate over all other possible conformers in gas-phase experiments for $n=8$ [15, 48].
- For $n=7$, the same qualitative picture emerges. Here, the next remaining conformer (Family 3) at 300 K is a mixed $3_{10}/\alpha$ -helix. The competing compact conformers (representatives of Family 2 and 2a) are significantly destabilized by $F_{harm.}(T)$.
- For $n=6$, the α -helix emerges as the room-temperature minimum free energy conformer, but the competing non-helical PES minimum, Family 1, remains close (50 meV).
- For $n=5$, the difference between the α -helix and Family 1 (g-1) decreases by 60 meV at 300 K, compared to the PES minimum, but Family 1 remains overall more favorable.

In essence, there is an uniform stabilization of helical over more compact (globular) structures as the temperature increases. The stabilization tendency increases with peptide length, confirming quantitatively and systematically from first principles the related observations in Refs. [13, 52, 53]. We next demonstrate that it is indeed the *vibrational entropy* term which is critical, and then pinpoint the physical reason among the low-frequency vibrational modes.

B. Origin of the entropic stabilization

In Fig. 2 we analyze the individual quantities composing the vibrational free energy differences between: Families 1 and 2 of $n=4$, Families 1 and the α -helical conformers of $n=5$ and 6, as well as Families 1 (α -helical) and 2 for $n=7$ and 8. The energy terms plotted are the PBE+vdW PES minimum energy, the harmonic internal energy (containing the zero-point energy) $\Delta U_{harm.}(T)$,

and the entropy term $TS_{harm.}(T)$. They are reported in Fig. 2 as energy differences, taking the non-helical conformer of each n as the reference, such that negative slopes correspond to a stabilization of the α -helices. Upon inspection of Fig. 2, we observe a monotonic stabilization of all helical conformers with increasing T . While for the shortest molecule ($n=4$) there is hardly any observable effect, the stabilization trend is enhanced with increasing length. For $n=6$, we predict a cross-over of the lowest-energy structures at $T \approx 150$ K. It is clear that among the individual contributions to the vibrational part of the free energy $F_{harm}(T)$, the entropy term $TS_{harm}(T)$ is indeed always the most important helix-favoring term. The zero-point-energy (ΔU_{harm} at $T=0$), is also favorable, but on a smaller scale.

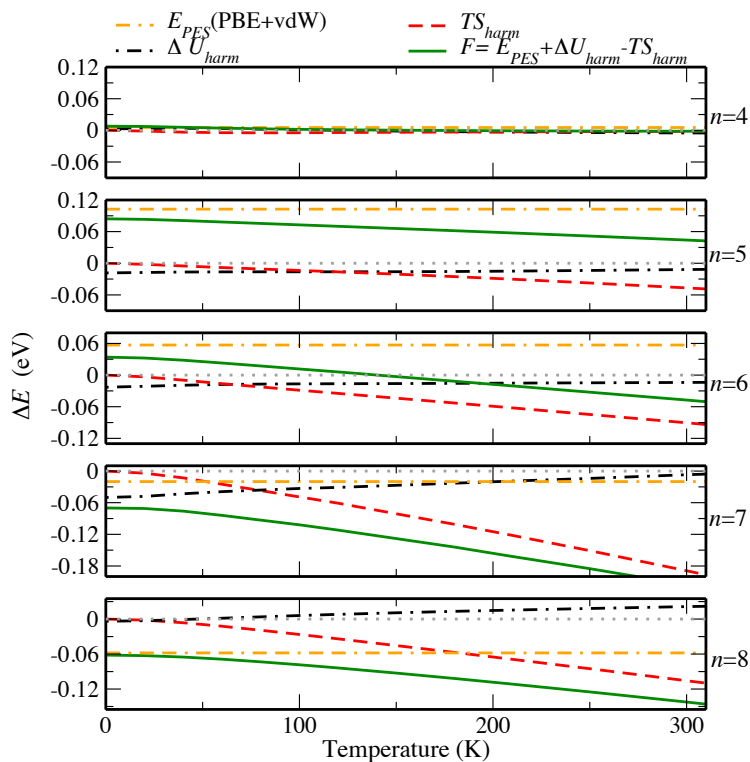


FIG. 2: Energy differences for each term of the harmonic free energies, as a function of temperature, for: Families 1 and 2 of $n=4$; Families 1 (g-1) and 2 (α) of $n=5$; Families 1 (“g-1” like) and 3 (α) of $n=6$; Families 1 (α) and 2 (compact) of $n=7$; and Families 1 (α) and 2 (compact) of $n=8$. In each case, the non- α -helical conformer was taken as the reference (i.e. negative slopes mean α -helix stabilization). The PBE+vdW energy differences are plotted with a yellow dash-dash-dot line, the harmonic internal energy $\Delta U_{harm.}$ as black dash-dot lines, the entropy term $TS_{harm.}$ as red dashed lines, and the sum $F_{harm.}$ as green full lines.

The observed stabilization of the α -helical conformers can be understood by analyzing the lowest-energy vibrational modes of different conformations. For simple helices, these modes have been

TABLE I: Position of the lowest vibrational mode, in cm^{-1} , for the lowest energy conformers of each family shown in Fig. 1 for $n=4-8$. We use red characters to indicate the α -helical conformers, a * symbol for the g-1-like conformers of $n=5$ and 6, and blue characters for the 3_{10} -helical conformer. The numerical accuracy of all computed frequencies is 2 cm^{-1} or better (See supplementary material).

length/conformer	4	5	6	7	8
Family 1	23	22*	20*	12	11
Family 1a	27	23	21	10	11
Family 1b	25	26			
Family 2	17	13	20	28	20
Family 2a			23	22	
Family 3	27*	20	8	15	16
Family 4	17		18	20*	15

estimated and analyzed before [65]. The important point here is that we have available a direct comparison against many other, non-helical structure candidates. These modes dominate in the harmonic free energy expression at room T , so that conformers with lower-frequency modes will effectively be stabilized over others. In Table I, the frequencies (in cm^{-1}) corresponding to the first normal modes of all conformers shown in Fig. 1 are reported. The lowest-energy α -helices, marked in red in Table I, show first vibrational normal modes between 8 cm^{-1} and 13 cm^{-1} . The same is true for families 1a of $n=7$ and 8, which only differ in details of the termination. In contrast, the conformers that have first vibrational modes of at least 20 cm^{-1} are all compact non-helical, for example: 28 cm^{-1} for Family 2 of $n=7$, and 22 cm^{-1} for Family 1 (g-1 motif) of $n=5$. The g-1 motif has the first vibrational mode lying around 20 cm^{-1} for $n=5, 6$, and 7 (marked with a * symbol in Table I).

Of course, the energy destabilization of the compact conformers with respect to the helices will depend not only on the first vibrational mode but also on the overall distribution of low-frequency modes. To illustrate this point, we show the frequencies of vibration lying between 0 and 50 cm^{-1} for Families 1 (α) and 2 (globular) of $n=7$ and 8 in Fig. 3(a) and (b). The α -helices have lower first vibrational normal modes, *and* have slightly higher (one or two modes) densities of modes in this region than the globular conformers.

Here, a comment regarding structures that are more elongated than α -helices is in order. It is customary to compare the stability of α -helices with 3_{10} helices and β -sheets or fully extended structures (e.g., in references [25, 26, 66–72] and many others). Following our rationale above, the

more extended the structure is, the softer the low vibrational modes will be. This indeed happens for the most extreme case, the fully extended structure (FES), where we find the first vibrational mode to lie around only 2 cm^{-1} (calculated for $n=8$ and 15). In fact, entropically stabilized β -sheets in *neutral* polyalanine in the gas-phase have been suggested in Ref. [33]. For 3_{10} helices, in our own structure searches for $n=4-8$, we find the first vibrational mode to lie always very close to their α -helical counterpart. Accordingly, it is the enthalpic energy difference that favors α -helices specifically over 3_{10} for all molecules studied. For infinite periodic structures, calculation of phonons and vibrational free energies for α -, 3_{10} -, and π -helices, and the FES in Ref. [66] corroborate our results. There, all helices are destabilized with respect to the FES at 300 K. The π -helix, which is the most compact among the helices studied in Ref. [66], is most destabilized by the vibrational entropy term.

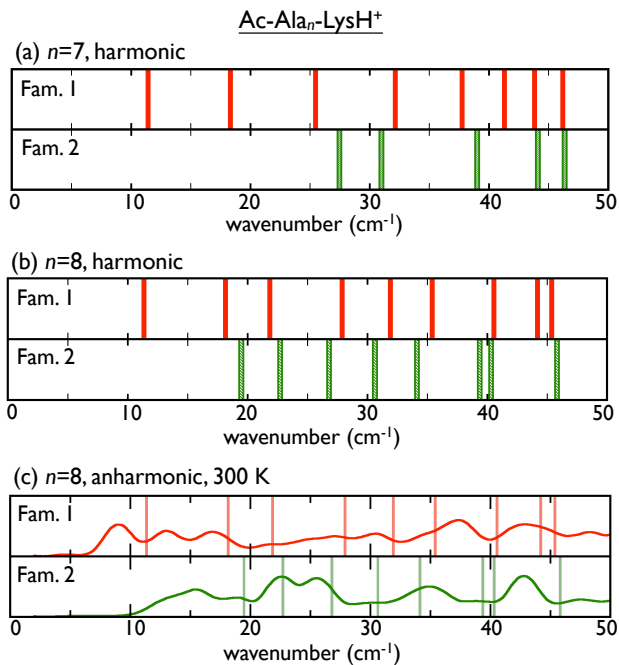


FIG. 3: Vibrational normal modes with frequencies up to 50 cm^{-1} for (a) Family 1 (α) and Family 2 (globular) of Ac-Ala₇-LysH⁺ and (b) Family 1 (α) and Family 2 (globular) of Ac-Ala₈-LysH⁺. (c) Vibrational density of states taken from the velocity autocorrelation function of 21ps of microcanonical AIMD at $\langle T \rangle = 300 \text{ K}$, for Family 1 (α) and Family 2 (globular) of Ac-Ala₈-LysH⁺. Light colored bars in (c) correspond to the harmonic normal frequencies of vibration [same as (b)].

1. *Beyond the harmonic approximation: Ab initio molecular dynamics*

We next show that the observations discussed in the last paragraph should hold also in a fully anharmonic picture. Even at relatively low temperature, where the structure still stays generally constant, we expect first the inherent anharmonicity of the local, nearly harmonic PES, then the lowest-barrier transitions between basins (side chain rotations), and then transitions between locally different backbone conformations and H-bond networks [16, 73] to contribute. Unfortunately, a direct calculation of these terms (e.g., by thermodynamic integration) is computationally prohibitive in DFT. We can, however, use explicit *ab initio* molecular dynamics simulations to gain some insights. In Fig. 3(c), we compare the Fourier-transformed velocity autocorrelation functions of the Family 1 (helical) and Family 2 (compact non-helical) conformers of $n=8$, extracted from explicit microcanonical *ab initio* molecular dynamics simulations (21 ps total time, 1 fs time step, initially thermalized to approximately room temperature). The Fourier transform of the velocity autocorrelation function corresponds to a vibrational density of states (VDOS). At $T=0$ and for classical nuclei, the autocorrelation function should reflect only the harmonic eigenmodes of Fig. 3(b). Compared to these modes, the onset of the calculated VDOS at $T\approx 300$ K is noticeably shifted towards lower frequencies for both conformers, but the onset frequency for the helix is still significantly lower than for the non-helical structure. Thus, the lower vibrational frequencies of the helix are also carried over to the full (anharmonic) motion of the conformers. In addition, the integral over the VDOS up to 50 cm^{-1} is 4% larger for the α -helical Family 1 than for the compact Family 2, i.e., the general downshift of frequencies in this region is also preserved.

Regarding the overall local structure stability during the AIMD simulation, we observe that the H-bond pattern of Family 2 (compact non-helical) stays essentially the same throughout the entire simulation (see Figure S.1 in the Supporting Information). In contrast, Family 1 displays local structural fluctuations in the helical part, occasionally forming short-lived 3_{10} -like H-bond connections. Similar fluctuations also occur in simulations of longer helices (e.g., Ac-Ala₁₅-LysH⁺ in Ref. [46]). It seems plausible that the overall greater “floppiness” of the helix compared to the more compact non-helical H-bond network adds another favorable entropic contribution at room temperature. This direct observation that we make has been guessed as the motive for the loss in entropy observed in α -helical formation, compared to a PPII helical structure in Ref. [70]. According to our reasoning, the PPII structure, being less compact than the α -helices should indeed show more fluctuations, just like α -helices do if compared to more compact conformers.

C. The role of the termination

Finally, we show that, especially for the short peptides considered here, there are two independent aspects to the stabilization of helical conformers: length and termination. To isolate their role, we examine the character of the lowest-frequency modes as a function of peptide length (also for longer helices) for two different terminations. The first is the LysH⁺-terminated series, which is the main subject of this work. We contrast this series with Li⁺-terminated polyalanine molecules Ala_n-Li⁺, a much more rigid termination as we shall see. For the latter, we assume α -helices for all n (fully relaxed in DFT-PBE+vdW), which are at least locally stable when Li⁺ is placed in contact with the last three residues at the C terminus. In Fig. 4(a), we compare the position of the first and second vibrational modes of these α -helical geometries of Ala_n-Li⁺, $n=5-15$, and 20, with the α -helical geometries of Ac-Ala_n-LysH⁺, $n=5-15$, and 19. For both peptide series, there is a monotonic decrease of the first and second vibrational frequencies for $n \geq 7$, but the starting point is much higher for the Li⁺ termination (26 cm⁻¹ at $n=7$) than for the LysH⁺ termination. A softening trend of the respective modes in neutral polyalanine helices with increasing length has also been observed in Ref. [65]. In order to characterize this vibrational mode in more detail, Fig. 4(b) visualizes the displacement of the backbone atoms of Ac-Ala₁₉-LysH⁺ when deforming this molecule along the first vibrational mode. Fig. 4(c) shows the relative length changes of the hydrogen bonds in the structure upon deformation along this mode. Subfigures (d) and (e) show the equivalent data for Ala₂₀-Li⁺. For both molecules, the vibration spans the helical part of the structures. For the LysH⁺ terminated molecule, we show that the actual LysH⁺ termination (connected to the last four CO residues) is clearly involved in the vibration. In contrast, the hypothetical Li⁺ charged termination constrains especially the C terminus to be much more rigid, as evidenced by the almost zero change of all Li-O distances. Here, the N-terminus is much more involved in the lowest-frequency modes. The same trends are observed for the smaller molecules in both series. Movies containing 3D visualizations of the first vibrational modes for helical and compact structures are contained in the Supporting Information. We thus conclude two points:

- (i) Helices are entropically favored by allowing delocalized, soft low-frequency modes that we do not observe in competing, more compact conformers of the same LysH⁺ termination (evidenced by Table I).
- (ii) For short conformers, the already electrostatically favorable LysH⁺ termination [29, 32] is additionally helpful by allowing soft, delocalized modes to include the termination also for short conformers, in contrast to the hypothetical, much harder charged termination by Li⁺. For long

enough helices these softer low frequency modes should exist regardless of the termination.

IV. CONCLUSIONS

In summary, we show from first principles, quantitatively, and for a particularly well studied series of polyalanine peptides how helices emerge with length and temperature as the leading structural pattern from a vast array of possible competing conformers. The crossover to helical stability with length is already apparent based on local structural minima of the potential-energy surface alone, due to the critical role of H-bond networks including their cooperativity [23–27] as well as that of vdW terms [27]. In addition, the contribution from softer low-frequency vibrational modes acts to stabilize helices with increasing temperature over their more compact competition. The specific experimental claim [15] of exclusively helical conformers at and above $n=8$ is thus explained by *both* enthalpic and entropic effects acting together at finite temperature. *Ab initio* molecular dynamics simulations corresponding to approximately room temperature suggest that these trends are further strengthened by anharmonic effects.

The emergence of room-temperature helix stability with length in Ac-Ala $_n$ -LysH $^+$ is thus the result of a subtle balance of enthalpic and entropic terms. In a non-vacuum environment, further terms would obviously contribute, but we expect the fact that helices, in general, allow locally softer vibrational modes to hold. Regarding the overall ubiquity of the helical motif in folded peptides and proteins, at least, we here show that low-frequency modes will be a significant quantitative contribution.

V. ACKNOWLEDGEMENT

The authors would like to acknowledge Dr. Carsten Baldauf for numerous helpful discussions and suggestions about the figures and paper in general, including the schematic backbone vibration visualization in Fig. 4.

VI. SUPPLEMENTAL INFORMATION

Additional computational details, XYZ geometries of conformers discussed in this paper, detailed information about the structures discussed in this paper, and movies illustrating the first vibrational

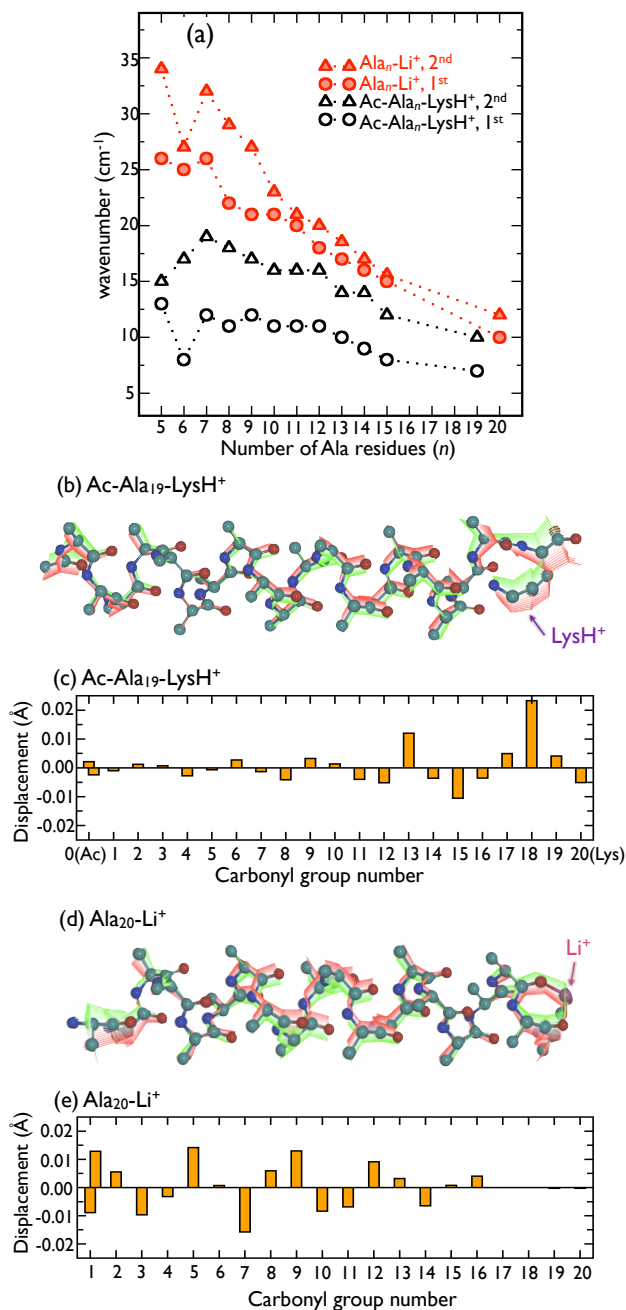


FIG. 4: Characterization of the lower vibrational modes of helices considered in this work. (a) Positions of the first and second vibrational modes of α -helical geometries of $\text{Ala}_n\text{-Li}^+$, $n=5-15$, and 20 (red) and α -helical geometries of $\text{Ac-Ala}_n\text{-LysH}^+$, $n=5-15$, and 19 (black). The accuracy of these numbers is of around 2 cm^{-1} . (b) Displacement caused on the backbone atoms of $\text{Ac-Ala}_{19}\text{-LysH}^+$ by deforming this molecule in the direction of the first vibrational mode, with red shaded areas corresponding to positive displacements and green shaded areas to negative displacements (hydrogen atoms not shown). (c) Relative change in H-bond distance when displacing 1 (normalized) unit of the first normal mode for $\text{Ac-Ala}_{19}\text{-LysH}^+$. We number the carbonyl groups from the N-terminus to the C-terminus. (d) Same as (b) for $\text{Ala}_{20}\text{-Li}^+$. (e) Same as (c) for $\text{Ala}_{20}\text{-Li}^+$ (in this case the last three carbonyl groups do not make H-bonds, but are connected to the Li^+ ion).

modes of helices and compact conformers.

- [1] Pauling, L.; Corey, R.; Branson, H. *Proc. Natl. Acad. Sci. USA* **1951**, *37*, 205–211.
- [2] Berman, H.M.; *et al.* *Nucl. Acids Res.* **2000**, *28*, 235–242. <http://www.pdb.org>.
- [3] Creighton, T.E. *Nature* **1987**, *326*, 547–548.
- [4] Pace, N.; Scholtz, J.M. *Biophys. J.* **1998**, *75*, 422–427.
- [5] Scholtz, J.M.; York, E.J.; Stewart, J.M.; Baldwin, R.L. *J. Am. Chem. Soc.* **1991**, *113*, 5102–5104.
- [6] Horovitz, A.; Matthews, J.M.; Fersht, A.R. *J. Mol. Biol.* **1992**, *227*, 560–568.
- [7] Creamer, T.P.; Rose, G.D. *Proc. Natl. Acad. Sci.* **1992**, *89*, 5937–5941.
- [8] Kinnear, B.; Jarrold, M. *J. Am. Chem. Soc.* **2001**, *123*, 7907–7908.
- [9] Miller, J.; Kennedy, R.; Kemp, D. *J. Am. Chem. Soc.* **2002**, *124*, 945–962.
- [10] Scott, K.A.; Alonso, D.V.; Sato, S.; Fersht, A.R.; Daggett, V. *Proc. Nat. Acad. Sci.* **2007**, *104*, 2661–2666.
- [11] Moreau, R.; *et al.* *J. Am. Chem. Soc.* **2009**, *131*, 13107–13116.
- [12] Zimm, B.H.; Bragg, J.K. *J. Chem. Phys.* **1959**, *31*, 526–535.
- [13] Kinnear, B.; Hartings, M.; Jarrold, M. *J Am Chem Soc* **2002**, *124*, 4422–4431.
- [14] Hudgins, R.R.; Ratner, M.A.; Jarrold, M.F. *J. Am. Chem. Soc.* **1998**, *120*, 12974–12975.
- [15] Kohtani, M.; Jarrold, M. *J. Am. Chem. Soc.* **2004**, *126*, 8454–8458.
- [16] Tournier, A.L.; Smith, J.C. *Phys. Rev. Lett.* **2003**, *91*, 208106.
- [17] Brooks, B.; Karplus, M. *Proc. Natl. Acad. Soc.* **1985**, *82*, 4995–4999
- [18] Editorial, Nature Chemistry Focus issue *Of polemics and progress*, *Nature Chem.* **2012**, *4*, 141.
- [19] Hay, S.; Scrutton, N.S. *Nature Chem.* **2012**, *4*, 161–168.
- [20] Glowacki, D.R.; Harvey, J.N.; Mulholland, A.J. *Nature Chem.* **2012**, *4*, 169–176.
- [21] Scholtz, J.M.; Baldwin, R.L. *Annu. Rev. Biophys. Biomol. Struct.* **1992**, *21*, 95–118, and references therein.
- [22] Baldwin, R.L. *J. Mol. Biol.* **2007**, *371*, 283–301.
- [23] Guo, H.; Karplus, M. *J. Phys. Chem.* **1994**, *98*, 7104–7105.
- [24] Baldwin, R.L. *J. Biol. Chem.* **2003**, *278*, 17581–17588.
- [25] Ireta, J.; Neugebauer, J.; Scheffler, M.; Rojo, A.; Galván, M. *J. Phys. Chem. B* **2003**, *107*, 1432–1437.
- [26] Wieczorek, R.; Dannenberg, J.J. *J. Am. Chem. Soc.* **2004**, *126*, 14198–14205.
- [27] Tkatchenko, A.; Rossi, M.; Blum, V.; Ireta, J.; Scheffler, M. *Phys. Rev. Lett.* **2011**, *106*, 118102.
- [28] Blagdon, D.E.; Goodman, M. *Biopolymers* **1975**, *14*, 241–245.
- [29] Presta, L.G.; Rose, G.D. *Science* **1988**, *240*, 1632–1641.
- [30] Serrano, L.; Fersht, A.R. *Nature* **1989**, *342*, 296–299.
- [31] Takahashi, S.; Kim, E.H.; Hibino, T.; Ooi, T. *Biopolymers* **1989**, *28*, 995–1009.

- [32] Marqusee, S.; Robbins, V.; Baldwin, R. *Proc. Natl. Acad. Sci.* **1989**, 86, 5286–5290.
- [33] Dugourd, P.; Antoine, R.; Breaux, G.; Broyer, M.; Jarrold, M. *J. Am. Chem. Soc.* **2005**, 127, 4675–4679.
- [34] Williams, L.; Kristian, K.; Kemp, D. *J. Am. Chem. Soc.* **1998**, 120, 11033–11043.
- [35] Hua, S.; Xu, L.; Li, W.; Li, S. *J. Phys. Chem. B* **2011**, 115, 11462–11469.
- [36] Liu, D.; Wyttenbach, T.; Bowers, M. *Int. J. Mass Spectrom.* **2004**, 236, 81–90.
- [37] Job, G.E.; *et al.* *J. Am. Chem. Soc.* **2006**, 128, 8227–8233.
- [38] Elstner, M.; Jalkanen, K.J.; Knapp-Mohammady, M.; Frauenheim, T.; Suhai, S. *Chem. Phys.* **2000**, 256, 15–27.
- [39] Salvador, P.; Asensio, A.; Dannenberg, J.J. *J. Phys. Chem. B* **2007**, 111, 7462–7466.
- [40] García A.E.; Sanbonmatsu, K.Y. *Proc. Natl. Acad. Sci.* **2002**, 99, 2782–2787.
- [41] Tirado-Rives, J.; Maxwell, D.S.; Jorgensen, W.L. *J. Am. Chem. Soc.* **1993**, 115, 11590–11593.
- [42] Kauzmann, W. *Adv. Protein Chem.* **1959**, 14, 1–63.
- [43] MacKenzie, K.R.; Prestegard, J.H.; Engelman, D.M. *Science* **1997**, 276, 131–133.
- [44] Khutorsky, V. *Biochem. Biophys. Res. Commun.* **2003**, 301, 31–34.
- [45] Jarrold, M. *Phys. Chem. Chem. Phys.* **2007**, 9, 1659–1671, and references therein.
- [46] Rossi, M.; *et al.* *J. Phys. Chem. Lett.* **2010**, 1, 3465–3470.
- [47] Kohtani, M.; Jones, T.; Schneider, J.; Jarrold, M. *J. Am. Chem. Soc.* **2004**, 126, 7420–7421.
- [48] Hu, Q.; Wang, P.; Laskin, J. *Phys. Chem. Chem. Phys.* **2010**, 12, 12802–12810.
- [49] Brooks, C.; Karplus, M.; Pettitt, M. *Proteins, Advances in Chemical Physics* (Wiley-VCH) **1988** 1st edition, 71, 180–183.
- [50] Poulain, P.; Calvo F.; Antoine R.; Broyer M.; Dugourd Ph. *Europhys Lett* **2007** 79, 66003.
- [51] Counterman, A.; Clemmer, D. *J. Phys. Chem. B* **2003** 107, 2111–2117.
- [52] Ma, B.; Tsai, C.J.; Nussinov, R. *Biophys J* **2000**, 79, 2739–2753.
- [53] Plowright, R.J.; Gloaguen, E.; Mons, M. *ChemPhysChem* **2011**, 12, 1889–1899.
- [54] Grimme, S. *J. Comput. Chem.* **2006**, 27, 1787–1799.
- [55] Chakrabartty, A.; Baldwin, R.L. *Adv. Protein Chem.* **1995**, 46, 141–176.
- [56] Perdew, J.P.; Burke, K.; Ernzerhof, M. *Phys. Rev. Lett.* **1996**, 77, 3865–3868.
- [57] Tkatchenko, A.; Scheffler, M. *Phys. Rev. Lett.* **2009**, 102, 073005.
- [58] Rossi, M. *Ab initio study of alanine-based polypeptide secondary-structure motifs in the gas phase*, Ph.D. thesis (Fritz-Haber-Institut der Max-Planck-Gesellschaft and Technische Universität Berlin), **2011**, <http://opus.kobv.de/tuberlin/volltexte/2012/3429/>.
- [59] McLean, J.; *et. al.* *J. Phys. Chem. B* **2010**, 114, 809–816
- [60] Wiczorek, R.; Dannenberg, J. *J. Am. Chem. Soc.* **2004**, 126, 12278–12279
- [61] Kaminski, G.A.; Friesner, R.A.; Tirado-Rives, J.; Jorgensen, W.L. *J. Phys. Chem. B* **2001**, 105, 6474–6487.
- [62] Ponder, J. *Tinker - software tools for molecular design*. In this work we used versions 4.2 and 5.1 of

the program and the force-fields' versions distributed within the package.

- [63] Blum, V.; *et al.* *Comp. Phys. Comm.* **2009**, 180, 2175–2196.
- [64] Havu, V.; Blum, V.; Havu, P.; Scheffler, M. *J. Comput. Phys.* **2009**, 228, 8367–8379.
- [65] Itoh, K.; Ikeda, A.; Iwamoto, T.; Nishizawa, S. *J. Molec. Struct.* **2011**, 1006, 52–58.
- [66] Ismer, L.; Ireta, J.; Neugebauer, J. *J. Phys. Chem. B* **2008**, 112, 4109–4112.
- [67] Improta, R.; Barone, V.; Kudin, K.; Scuseria, G. *J. Am. Chem. Soc.* **2001**, 123, 3311–3322.
- [68] Topol, I.; *et. al.*, *J. Am. Chem. Soc.* **2001**, 123, 6054–6060.
- [69] Wu, Y.-D.; Zhao, Y.-L. *J. Am. Chem. Soc.* **2001**, 123, 5313–5319
- [70] Shi, Z.; Olson, C.; Rose, G.; Baldwin, R.; Kallenbach, N. *Proc. Nat. Acad. Sci.* **2002**, 99, 9190–9195.
- [71] Bour, P.; Kubelka, J.; Keiderling, T. *Biopolymers* **2002**, 65, 45–59.
- [72] Penev, E.; Ireta, J.; Shea J-E. *J. Phys. Chem. B* **2008**, 112, 6872–6877.
- [73] Hong, L.; Smolin, N.; Lindner, B.; Sokolov, A.P.; Smith, J.C. *Phys. Rev. Lett.* **2011**, 107, 148102.
- [74] The free energy contributions from rigid-body rotations are also included, but differences between these energies for different conformers were found to be of the order of only a few meV, with the maximum difference amounting to 8 meV.